Z. Physik 237, 189–204 (1970)

Energy Levels and Interaction between Eu^{3+}-ions at Lattice Sites of Symmetry C_2 and Symmetry C_{3i} in Y_2O_3

J. HEBER, K. H. HELLWEGE, U. KÖBLER and H. MURMANN
Institut für Technische Physik, Technische Hochschule, Darmstadt

Received June 8, 1970

Besides the known energy levels of Eu^{3+} at lattice sites of symmetry C_2 in Y_2O_3, some transitions of this ion at lattice sites of symmetry C_{3i} in the same host crystal have been found and it was possible to construct the energy level scheme in part. Evidence for an energy transfer from $Eu^{3+}(C_{3i})$ to $Eu^{3+}(C_2)$ is given, the strength of which is measured as a function of the Eu_2O_3 concentration. The results lead to the assumption of a fixed distance R_0 for the interaction responsible for the energy transfer. A temperature-independent value of $R_0 = 8.7$ Å was found. The full explanation of the underlying quantum mechanical mechanism requires further experiments.

Introduction

There are two crystallographically different Y^{3+} lattice sites in the diamagnetic host crystal Y_2O_3, which possess the point symmetries C_2 and C_{3i}[1,2]. It is well known from paramagnetic resonance studies, that the trivalent rare earth ions occupy both the C_2 and C_{3i} lattice sites with nearly equal probability[3-5]. Thus Y_2O_3 doped with Eu_2O_3 provides two ion systems, which will be called $Eu^{3+}(C_2)$ and $Eu^{3+}(C_{3i})$.

Since there is no center of symmetry at lattice sites of symmetry C_2, the parity of the $4f^6$ electron wave functions is not defined. The intensities of the optical transitions within the $4f^n$ configuration are mainly due to electric dipole transitions $E1$, which are forced by the odd parity parts of the crystalline electric field. These $E1$ type transitions are in general far stronger than the magnetic dipole transitions $M1$, despite the fact that the latter are allowed in the free ion case. Furthermore, there are no strict angular momentum selection rules for $E1$ type tran-

---

[1] Gschneidner, K. A.: Rare-earth alloys, p. 242. Princeton, N. J.: D. van Nostrand 1961.

[2] Pauling, L., Shappell, M. D.: Z. Kristallographie **75**, 128 (1930).

[3] Mandel, M.: Appl. Phys. Letters **2**, 197 (1963).

[4] Schäfer, G.: Phys. kond. Materie **9**, 359 (1969).

[5] Pastor, R. C., Kimura, H., Podoksik, L., Cernichiari, O., Pearson, M. A.: J. Chem. Phys. **48**, 3830 (1968).

sitions in systems with low symmetries, so that for the system $Eu^{3+}(C_2)$ all transitions should be observable.

At lattice sites of symmetry C_{3i} the parity of the electron wave functions is an exact quantum number (for $4f^6$ it is even). In this case only magnetic dipole transitions $M1$, electric quadrupole transitions $E2$ or higher multipole radiation of even parity should be observed. But since we find that the selection rule

$$\Delta J=0, \pm 1; \quad (J=0 \rightarrow J=0 \text{ forbidden}) \qquad (1)$$

always holds, we can be sure that pure magnetic dipole transitions are being observed. This selection rule for $M1$ type transitions of the free ion holds in a crystalline environment as well if J is a good quantum number, i.e. if the crystal-field splitting is small compared with the spin-orbit splitting. This condition is always true in the case of rare earth ions in crystalline electric fields.

It has been proved by Deutschbein[6] that Eu^{3+} exhibits very intense magnetic dipole radiation in the $^7F \rightarrow {}^5D$ transitions, so that some fluorescence and absorption transitions of this ion should be observable at lattice sites which possess a center of symmetry. In their absorption spectrum of Y_2O_3/Eu_2O_3 Chang and Gruber[7] have found within the $^7F_0 \rightarrow {}^5D_1$ transitions two extra lines in addition to the three expected for the system $Eu^{3+}(C_2)$ alone. This can be readily explained by supposing that two lines belong to $Eu^{3+}(C_{3i})$ and three lines to $Eu^{3+}(C_2)$, which are the correct numbers for $J=1$ states under the symmetries C_{3i} and C_2 respectively.

Forest and Ban[8] have shown how to distinguish which of these five absorption lines are $^7F_0 \rightarrow {}^5D_1$ $Eu^{3+}(C_{3i})$ and which are $^7F_0 \rightarrow {}^5D_1$ $Eu^{3+}(C_2)$ transitions. Furthermore they found two fluorescence lines which they assigned as $^5D_0 \rightarrow {}^7F_1$ $Eu^{3+}(C_{3i})$ transitions. This can be done by comparing the fluorescence decay times of corresponding transitions of both ion types. Of the two possible radiative decay mechanisms $E1$ and $M1$ only the latter will occur at lattice sites with symmetry C_{3i} thus leading to a longer fluorescence lifetime for $Eu^{3+}(C_{3i})$. This is in accordance with the experiments where we have found a lifetime of (7.77 ± 0.1) msec for the $^5D_0$ $Eu^{3+}(C_{3i})$ fluorescence and (1.00 ± 0.01) msec for $^5D_0$ $Eu^{3+}(C_2)$, both at $T=77$ °K. These values agree well with theoretical predictions[9].

The aim of this work is twofold: 1. to construct the energy level scheme of $Eu^{3+}(C_{3i})$ from the spectroscopic data available, and 2. to

---

[6] Deutschbein, O.: Ann. Phys. (5), **36**, 183 (1939).

[7] Chang, N. C., Gruber, J. B.: J. Chem. Phys. **41**, 3227 (1964).

[8] Forest, H., Ban, G.: J. Electrochem. Soc. **116**, 474 (1969).

[9] Weber, M. J.: Phys. Rev. **171**, 283 (1968).

investigate quantitatively the energy transfer from Eu^{3+} (C_{3i}) to Eu^{3+} (C_2) which has already been stated qualitatively by Forest and Ban[8]. The system Y_2O_3/Eu_2O_3 seems quite appropriate for such investigations because here one is dealing with well defined systems of similar acceptors and donors.

Experimental

Y_2O_3 belongs to be cubic space group T_h^7 (1, 2). The unit cell is a cube and contains 16 formula units. Eight of the 32 Y^{3+} lattice sites possess the point symmetry C_{3i} with the threefold axes parallel to the body diagonals of the unit cell, and the remaining 24 possess the point symmetry C_2 with the twofold axes parallel to the edges of the unit cell.

Our Verneuil-grown crystals were optically clear and about 10 mm long and 3 to 4 mm in diameter. The starting materials were 99.9999% pure Y_2O_3 and 99.999% pure Eu_2O_3. Fluorescence and absorption spectra were recorded photoelectrically with a 1 m Czerny-Turner spectrograph of Jarrell-Ash, equipped with a grating with 1,180 grooves/mm. For the observation of the fluorescence spectra a high pressure 1,000 Watt xenon lamp served as wide band excitation source in conjunction with appropriate UV filters. Absorption spectra were recorded using a 150 Watt quartz-iodine lamp as the light source. The excitation spactra were recorded by passing the exciting light through the 1 m Czerny-Turner spectrograph and observing the fluorescence through a 0.2 m monochromator with a grating with 2,160 grooves/mm. The crystals were immersed in liquid nitrogen or liquid helium for the low temperature measurements.

Energy Levels of Eu^{3+} (C_{3i})

Only at concentrations $c \leqq 0.1$ mol% Eu_2O_3, when the Eu^{3+}-ions are remote enough from each other so that no interaction takes place between them, does there really exist two independent ion systems $Eu^{3+}(C_{3i})$ and $Eu^{3+}(C_2)$.

Provided that this is true, and that the single ion model holds, one can separate the transitions of the two systems as follows. At symmetry sites C_2 all $2J+1$ crystal field components of the $^7F_0 \rightarrow {}^5D_J$ transitions should be observable, but on lattice sites of symmetry C_{3i} only the two $^7F_0 \rightarrow {}^5D_1$ lines should appear according to the selection rule (1). This is indeed the case since nowhere else more than $2J+1$ lines were found in absorption from the $^7F_0$ ground state to any other ^5D_J level. For the sake of separating the five $^7F_0 \rightarrow {}^5D_1$ absorption lines into C_{3i} and C_2 transitions one has to compare the fluorescence spectra taken under monochromatic excitation into each of these lines separately. Only C_{3i} lines should appear in the fluorescence spectrum when one is exciting

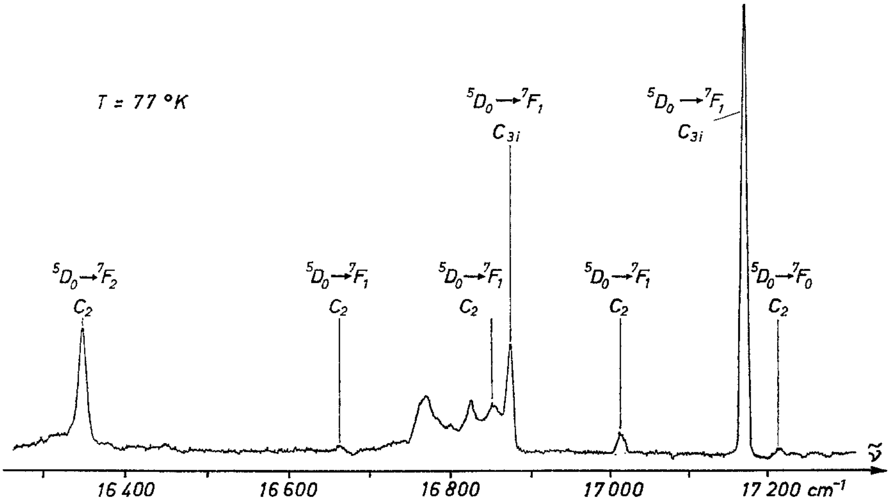

Fig. 1. Fluorescence spectrum of a crystal with 0.5 mol % Eu_2O_3 in Y_2O_3 at $T = 77$ °K recorded under narrow band excitation into $^7F_0 \rightarrow {}^5D_1$ Eu^{3+} (C_{3i}) at $\tilde{\nu} = 18{,}991\ cm^{-1}$, showing the two $^5D_0 \rightarrow {}^7F_1$ Eu^{3+} (C_{3i}) fluorescence lines. The broad lines at 16,800 cm^{-1} are vibronic transitions of Eu^{3+} (C_{3i})

into a Eu^{3+} (C_{3i}) transition. In this way one can not only distinguish between the $^7F_0 \rightarrow {}^5D_1$ absorption lines but also between fluorescence lines of the two ion types. In agreement with Forest and Ban[8] we found only two Eu^{3+} (C_{3i}) fluorescence lines, which are assigned as $^5D_0 \rightarrow {}^7F_1$ transitions because of their long fluorescence decay times [(7.77 ± 0.1) msec at 77 °K, for both lines].

Fig. 1 shows the fluorescence spectrum of a crystal doped with 0.5 mol% Eu_2O_3, recorded at 77 °K under monochromatic excitation into the C_{3i} absorption line with $\tilde{\nu} = 18{,}991\ cm^{-1}$. The two Eu^{3+} (C_{3i}) fluorescence lines are more prominent than in Fig. 2 where the same spectrum is recorded under UV excitation, in which case both ion-types are simultaneously excited.

From the system Eu^{3+} (C_{3i}) no further spectroscopic data other than the two $^7F_0 \rightarrow {}^5D_1$ absorption lines at $\tilde{\nu} = 18{,}991\ cm^{-1}$ and $\tilde{\nu} = 19{,}080\ cm^{-1}$ and the two fluorescence transitions $^5D_0 \rightarrow {}^7F_1$ at $\tilde{\nu} = 16{,}873\ cm^{-1}$ and $\tilde{\nu} = 17{,}170\ cm^{-1}$ were available. To construct the level scheme one of the following energy differences is needed to locate the $^5D_0$ or equivalently the $^7F_1$ level (see Fig. 4):

$$^5D_0 - {}^5D_1; \quad {}^7F_1 - {}^5D_1 \quad \text{or} \quad {}^7F_0 - {}^7F_1 .$$

Since the $^7F_1 \rightarrow {}^5D_0$ Eu^{3+} (C_{3i}) transition with $\tilde{\nu} = 17{,}170\ cm^{-1}$ is also seen in absorption between room temperature and approximately 100 °K

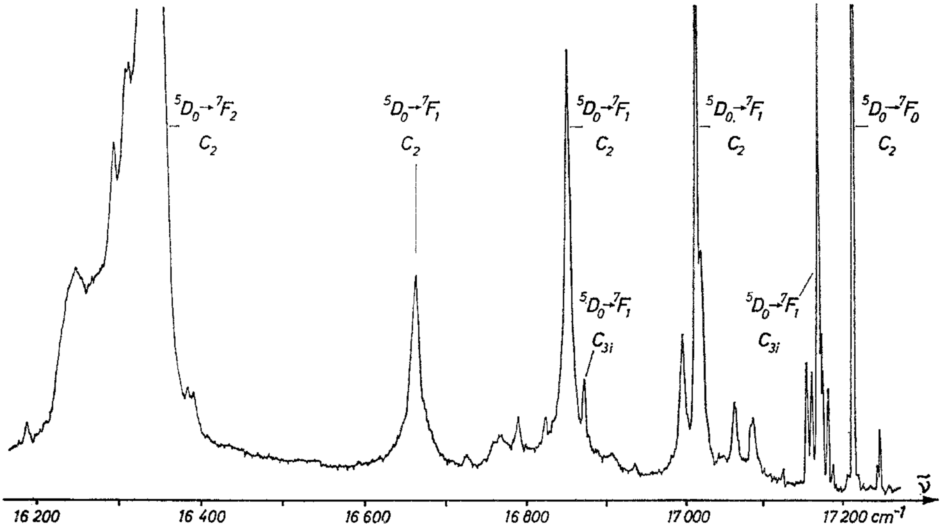

Fig. 2. Fluorescence spectrum of a crystal with $c = 0.5$ mol% Eu_2O_3 in Y_2O_3 at $T = 77$ °K recorded under UV excitation, where $Eu^{3+}(C_2)$ and $Eu^{3+}(C_{3i})$ are simultaneously excited

we have determined the $^7F_0 - ^7F_1$ energy distance ΔW_1 by measuring the temperature dependence of the absorption intensity of this line which is given by the product of the occupation number of the $^7F_1$ initial state and the transition probability. Assuming that the transition probability has a temperature-independent value w^*, one expects a Boltzmann-type temperature dependence

$$I_{\mathrm{Abs}}(T) \sim w^* \cdot \frac{1}{Z(T)} \cdot \exp\left(-\frac{\Delta W_1}{kT}\right)$$

where $Z(T)$ is the partition function. Since it is more convenient to compare the intensities of two lines than to measure their absolute intensities, we have compared the intensity of the C_{3i} line at $\tilde{\nu} = 17{,}170$ cm^{-1} with the intensity of the corresponding line of the system $Eu^{3+}(C_2)$ which originates from an excited level 201 cm^{-1} above the ground state and has an energy of $\tilde{\nu} = 17{,}014$ cm^{-1}. Thus the ratio of the two intensities is given by

$$\frac{I_{\mathrm{Abs}}(C_{3i})}{I_{\mathrm{Abs}}(C_2)} \sim \frac{Z(C_2)}{Z(C_{3i})} \cdot \exp\left(-\frac{\Delta W_1(C_{3i}) - \Delta W_1(C_2)}{kT}\right). \qquad (2)$$

The unknown energy $\Delta W_1(C_{3i})$ was determined by an iterative procedure because $Z(C_{3i})$ is also unknown.

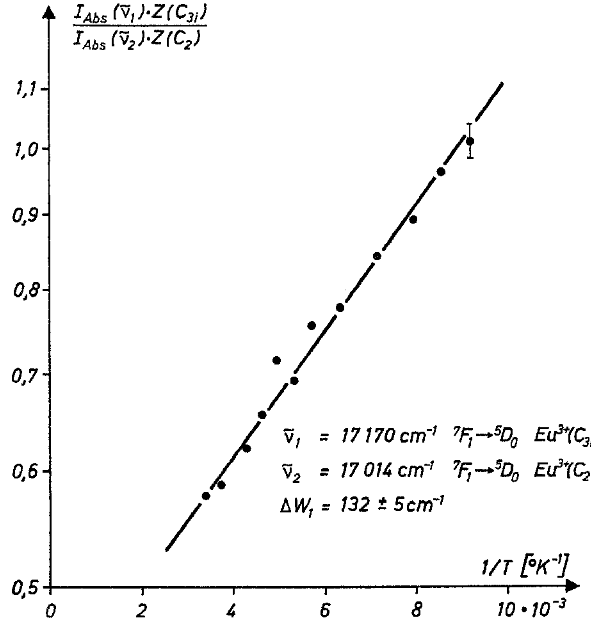

Fig. 3. Determination of the energy ΔW_1 of the first excited state $^7F_1$ of Eu$^{3+}(C_{3i})$ by comparison of the temperature dependence of the intensities of two absorption lines. The degeneracy of the energy level with $\Delta W_1 = 132$ cm^{-1} is twofold. $c = 5.0$ mol% Eu$_2$O$_3$ in Y$_2$O$_3$

For the first step only the first term (=1) in the partition functions of both ion types was retained

$$Z = \sum_{i=0}^{\infty} g_i e^{-\frac{\Delta W_i}{kT}}, \qquad g_0 = 1, \qquad \Delta W_0 = 0$$

where g_i is the degeneracy of the i-th level.

From this first step an approximate value of $\Delta W_1(C_{3i})$ of 120 cm^{-1} was found, by plotting (2) on a logarithmic scale. Then the known $Z(C_2)$ partition function was inserted in (2) and $Z(C_{3i})$ was approximated by

$$Z(C_{3i}) = 1 + g_1 e^{-\frac{\Delta W_1}{kT}} \tag{3}$$

for determining the degeneracy g_1 of the first excited state of Eu^{3+} (C_{3i}). Taking only the low temperature values, where (3) is a good approximation one gets $g_1 = 2$. Thus, knowing the splitting of the Eu^{3+} (C_{3i}) $^7F_1$ level from fluorescence data to be 297 cm^{-1}, one can also construct $Z(C_{3i})$ with the upper $^7F_1$ level being a singlet and taking into account only the contributions from the ground state $^7F_0$ and the excited state

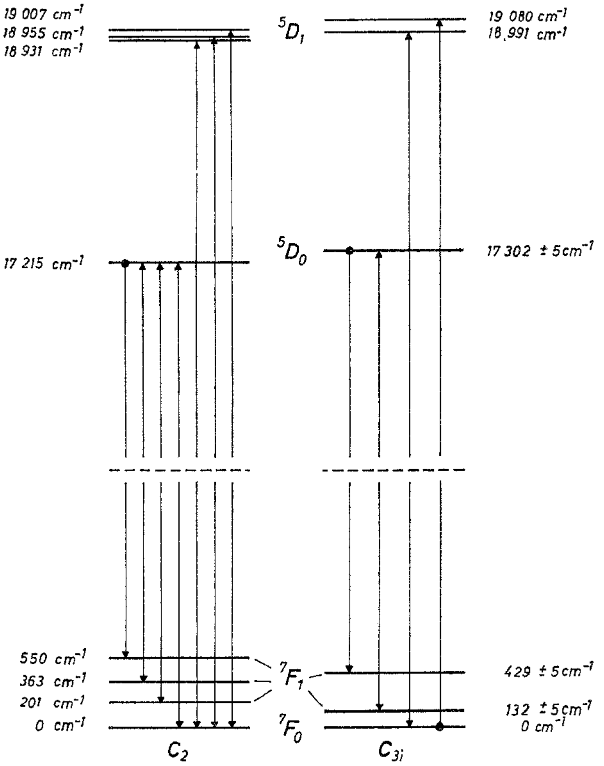

Fig. 4. Energy levels of corresponding states of $Eu^{3+}(C_2)$ and $Eu^{3+}(C_{3i})$ in Y_2O_3

$^7F_1$. Therefore plotting

$$\frac{I_{\mathrm{Abs}}(C_{3i})\cdot Z(C_{3i})}{I_{\mathrm{Abs}}(C_2)\cdot Z(C_2)} \sim e^{-\frac{\Delta W_1(C_{3i})-\Delta W_1(C_2)}{kT}} \tag{4}$$

on a logarithmic scale one can improve the value $\Delta W_1(C_{3i})$ and reevaluate $Z(C_{3i})$ until convergence is reached. The final value obtained is

$$\Delta W_1(C_{3i}) = 132 \pm 5\,\mathrm{cm}^{-1}$$

belonging to a twofold level. Fig. 3 shows the logarithmic plot of (4) as a function of the inverse absolute temperature and Fig. 4 the energy levels of the corresponding states of both ion types.

Energy Transfer from Eu^{3+} (C_{3i}) to Eu^{3+} (C_2)

To check the energy level scheme of Fig. 4 one can use the excitation spectra of the $^5D_0$ fluorescence, which show the variation of the fluorescence intensity of a given line as a function of the wavelength of the

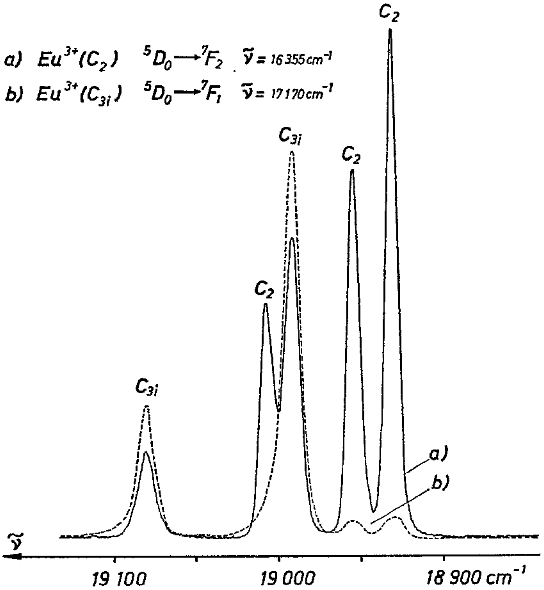

Fig. 5. The $^7F_0 \rightarrow {}^5D_1$ transitions in the excitation spectra of the a) $Eu^{3+}(C_2)$ fluorescence $^5D_0 \rightarrow {}^7F_2$; $\tilde{\nu} = 16{,}355$ cm^{-1}. b) $Eu^{3+}(C_{3i})$ fluorescence $^5D_0 \rightarrow {}^7F_1$; $\tilde{\nu} = 17{,}170$ cm^{-1}. $T = 77$ °K, $c = 5.0$ mol% Eu_2O_3 in Y_2O_3

exciting radiation. When the two ion types are isolated from each other, the excitation spectrum of the fluorescence of each species should contain only transitions due to this type. This is the fact only at concentrations with $c \leqq 0.1$ mol% Eu_2O_3. At higher concentrations $Eu^{3+}(C_{3i})$ transitions appear in the excitation spectrum of $^5D_0$ $Eu^{3+}(C_2)$. This is illustrated in Fig. 5, where the excitation spectrum of the strongest $^5D_0$ $Eu^{3+}(C_2)$ fluorescence line at $\tilde{\nu} = 16{,}355$ cm^{-1} is shown (by the solid line) in the region of the $^7F_0 \rightarrow {}^5D_1$ absorption transitions ($c = 5$ mol% Eu_2O_3, $T = 77$ °K).

In this spectrum the $^7F_0 \rightarrow {}^5D_1$ $Eu^{3+}(C_{3i})$ transitions also appear, indicating that one can excite the $^5D_0$ $Eu^{3+}(C_2)$ fluorescence by irradiating into the system $Eu^{3+}(C_{3i})$. This can only be explained by virtue of an energy transfer from $Eu^{3+}(C_{3i})$ to $Eu^{3+}(C_2)$. In the opposite direction from $Eu^{3+}(C_2)$ to $Eu^{3+}(C_{3i})$ the energy transfer is much weaker, as can be seen from the excitation spectrum of the $^5D_0$ $Eu^{3+}(C_{3i})$ fluorescence shown in Fig. 5 by the dotted line. The net energy transfer is therefore from $Eu^{3+}(C_{3i})$ to $Eu^{3+}(C_2)$, the former being the donors and the latter being the acceptors.

The intensity of the two $^7F_0 \rightarrow {}^5D_1$ $Eu^{3+}(C_{3i})$ transitions in the excitation spectrum of the $Eu^{3+}(C_2)$ fluorescence is a direct measure

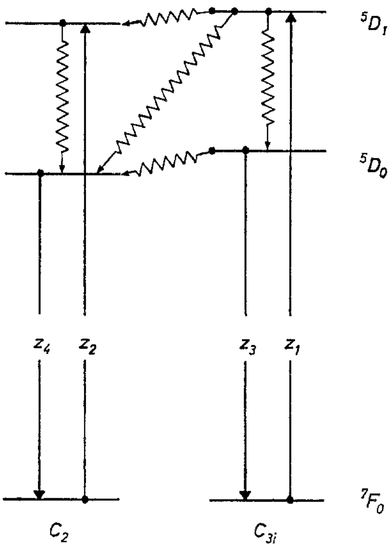

Fig. 6. z_1 number of photons absorbed in the $^5D_1$ level by the donors Eu^{3+}(C_{3i}). z_2 number of photons absorbed in the $^5D_1$ level by the acceptors Eu^{3+}(C_2). z_3 number of photons emitted from the $^5D_0$ of Eu^{3+}(C_{3i}). z_4 number of photons emitted from the $^5D_0$ of Eu^{3+}(C_2)

of the probability for energy transfer w_T which will be defined according to Fig. 6 as:

$$w_T = \left.\frac{z_4}{z_1}\right|_{z_2=0}. \tag{5}$$

w_T is therefore the quantum efficiency for the $^5D_0$ Eu^{3+} (C_2) fluorescence by pumping via the Eu^{3+} (C_{3i}) donors.

For practical reasons it is more convenient to define a new quantity w_T' which is easier to obtain by the experiment

$$w_T' = \left.\frac{z_4}{z_1}\right|_{z_2=0} \cdot \frac{1}{\left.\frac{z_4}{z_2}\right|_{z_1=0}} = \frac{z_4|_{z_2=0}}{z_4|_{z_1=0}} \cdot \left(\frac{z_1}{z_2}\right)^{-1} \tag{6a}$$

or using the definitions of quantum efficiencies of donors (d) and acceptors (a)

$$\eta_d = \left.\frac{z_3}{z_1}\right|_{z_2=0}, \qquad \eta_a = \left.\frac{z_4}{z_2}\right|_{z_1=0} \tag{7}$$

one gets

$$\eta_a \cdot w_T' = w_T. \tag{6b}$$

According to (6a) w'_T is the ratio of the fluorescence intensity of ${}^5D_0$ $\mathrm{Eu}^{3+}(C_2)$ obtained by exciting only into ${}^5D_1$ $\mathrm{Eu}^{3+}(C_{3i})$ divided by the intensity of the same fluorescence obtained by exciting only into ${}^5D_1$ $\mathrm{Eu}^{3+}(C_2)$ and normalized to the ratio of the ${}^5D_1$ absorption intensities of both ion types.

To determine w'_T experimentally one has to compare the areas under the two ${}^5D_1$ $\mathrm{Eu}^{3+}(C_{3i})$ lines with the areas under the three ${}^5D_1$ $\mathrm{Eu}^{3+}(C_2)$ lines in the excitation spectrum of the ${}^5D_0$ $\mathrm{Eu}^{3+}(C_2)$ fluorescence (Fig. 5) and to divide this ratio by the ratio of the intensities of the same lines in the absorption spectrum.

This is possible because the intensity of the strongest ${}^5D_0$ $\mathrm{Eu}^{3+}(C_2)$ fluorescence line observed here (${}^5D_0 \to {}^7F_2$; $\tilde{\nu}=16{,}355\ \mathrm{cm}^{-1}$) is proportional to the entire ${}^5D_0$ fluorescence intensity to within a constant which is independent of the excitation conditions.

The number of photons absorbed by a crystal (z_1, z_2) is proportional to

$$\int [I_0 - I(\tilde{\nu})]\, d\tilde{\nu} \tag{8}$$

where the integral is over the absorption line. I_0 is the incident intensity and $I(\tilde{\nu})$ is the transmitted intensity with

$$I(\tilde{\nu}) = I_0\, e^{-k(\tilde{\nu})\cdot d}$$

where d is the thickness of the crystal and $k(\tilde{\nu})$ the absorption constant. Only in the case of low optical thickness $(k_{\max}\cdot d \ll 1)$ there is a direct proportionality between (8) and the integrated absorption probability

$$\int k(\tilde{\nu})\, d\tilde{\nu} = \int n\cdot\sigma(\tilde{\nu})\, d\tilde{\nu} \tag{9}$$

where n is the density of ions and $\sigma(\tilde{\nu})$ the absorption cross-section.

We have measured the integrated absorption probabilities for the ${}^7F_0 \to {}^5D_1$ transition of both ion types and found a concentration-independent ratio at 77 °K of

$$\left.\frac{\int k(\tilde{\nu})\, d\tilde{\nu}(C_{3i})}{\int k(\tilde{\nu})\, d\tilde{\nu}(C_2)}\right|_{{}^7F_0\to{}^5D_1} = 0.36 \pm 0.01.$$

Since there are three times more C_2 lattice sites than C_{3i} lattice sites and the radiative transition probability of the Eu^{3+} ions at the former is expected to be greater than at the latter one would expect a ratio smaller than $\frac{1}{3}$.

This is contrary to the observation and may indicate that the Eu^{3+} ions favour the C_{3i} lattice sites slightly more than the C_2 lattice sites.

A second quantity which can characterize the energy transfer is the ratio of the ${}^5D_0$ $\mathrm{Eu}^{3+}(C_{3i})$ fluorescence intensity to the ${}^5D_0$ $\mathrm{Eu}^{3+}(C_2)$

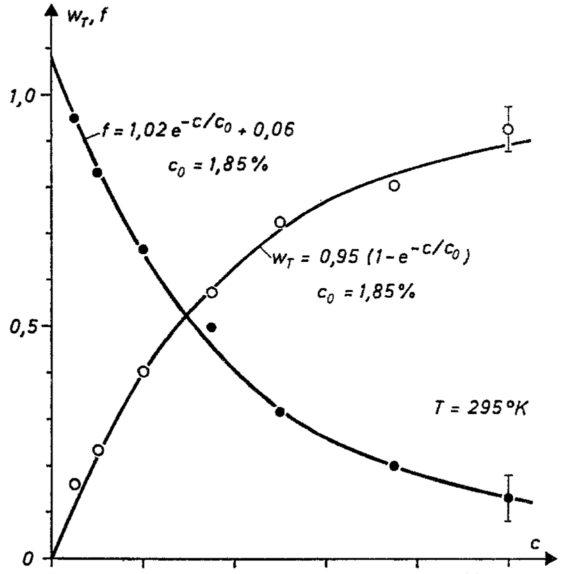

Fig. 7a. w_T probability for energy transfer from Eu^{3+}(C_{3i}) to Eu^{3+}(C_2). f ratio of the quantum efficiencies of the $^5D_0$ fluorescence of Eu^{3+}(C_{3i}) and Eu^{3+}(C_2) by exciting into $^5D_1$

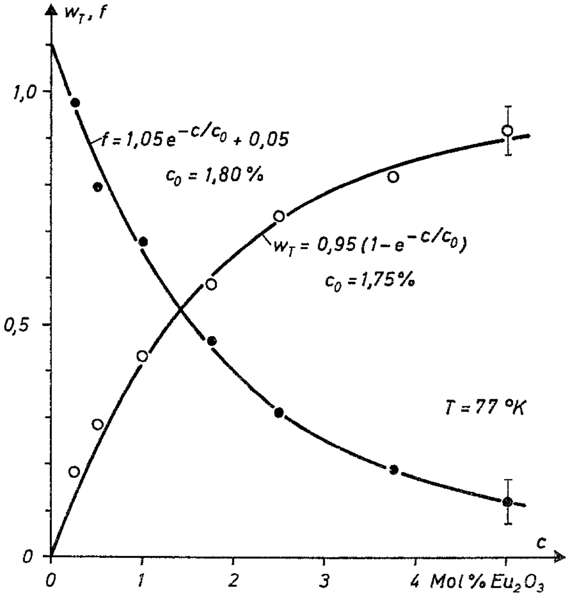

Fig. 7b. w_T probability for energy transfer from Eu^{3+}(C_{3i}) to Eu^{3+}(C_2). f ratio of the quantum efficiencies of the $^5D_0$ fluorescence of Eu^{3+}(C_{3i}) and Eu^{3+}(C_2) by exciting into $^5D_1$

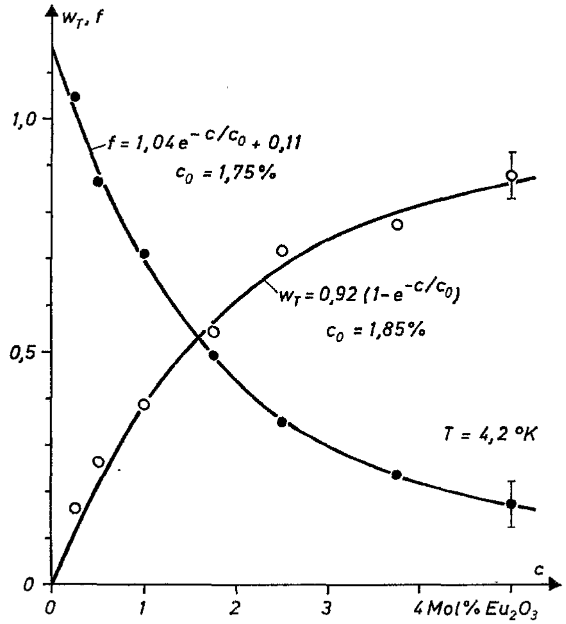

Fig. 7c. w_T probability for energy transfer from $Eu^{3+}(C_{3i})$ to $Eu^{3+}(C_2)$. f ratio of the quantum efficiencies of the $^5D_0$ fluorescence of $Eu^{3+}(C_{3i})$ and $Eu^{3+}(C_2)$ by exciting into $^5D_1$

fluorescence intensity normalized to the ratio of the corresponding absorption intensities of the exciting transition $^7F_0 \to {}^5D_1$ by simultaneous excitation of both ion types (Fig. 6).

$$f = \frac{z_3}{z_4} \cdot \frac{z_2}{z_1} = \frac{\eta_d}{\eta_a}. \tag{10}$$

The quantity f is equal to the ratio of the quantum efficiencies of both ion types.

Fig. 7a, 7b and 7c show the concentration dependence of the quantities w_T and f at the three temperatures 295, 77 and 4.2 °K.

The solid lines are optimum fits according to empirical functions of the form

$$w_T = A\left(1 - e^{-\frac{c}{c_0}}\right) \quad \text{and} \quad f = B\, e^{-\frac{c}{c_0}} + 1 - A \tag{11}$$

with the indicated values of the parameters A, B and c_0. How one gets w_T from the measured quantity w_T' will be explained in the following section.

Discussion of the Results

To explain the empirical relation (11) we propose a model in which a fixed range R_0 is adopted for the interaction responsible for the energy transfer. Whenever an acceptor ion is nearer to an excited donor ion than R_0, energy transfer will take place with a certain finite probability. This probability is assumed to be independent of the relativ distance of both ions within R_0. If the nearest acceptor ion is farther than R_0 from an excited donor ion, no energy transfer will occur.

In this case the concentration dependence of w_T is determined by the probability of finding an acceptor ion within a sphere with volume $\frac{4\pi}{3} R_0^3$ around a donor ion.

Taking a Poisson-type distribution, which means that one disregards the discrete lattice of the crystal and deals with a continuum with the same mean ion density, one gets

$$w_0 = e^{-\frac{4\pi}{3} R_0^3 \cdot n(C_2)}$$

for the probability of finding no $Eu^{3+}(C_2)$ acceptor ion within this sphere, where $n(C_2)$ is the density of the $Eu^{3+}(C_2)$ ions. The complementary probability of finding one or more $Eu^{3+}(C_2)$ ions in this sphere is therefore given by

$$w_1 = 1 - e^{-\frac{4\pi}{3} R_0^3 \cdot n(C_2)}.$$

Expressing the range of the interaction R_0 by an equivalent $Eu^{3+}(C_2)$ ion density according to

$$n_0(C_2) = \frac{1}{\frac{4\pi}{3} R_0^3}$$

one gets

$$w_1 = 1 - e^{-\frac{n}{n_0}} = 1 - e^{-\frac{c}{c_0}}$$

where c is the molar concentration of Eu_2O_3 in Y_2O_3. The probability for energy transfer w_T is then simply

$$w_T = A w_1 = A\left(1 - e^{-\frac{c}{c_0}}\right)$$

which is of the form (11) assumed empirically, where the constant A has to be determined by experiment.

To explain the concentration dependence of the quantity f one can make the following ansatz for the quantum efficiencies of the donors (index d) and acceptors (index a)

$$\eta_d = \eta_{d0} \cdot e^{-\frac{c}{c_0}} + \eta_{d\infty}\left(1 - e^{-\frac{c}{c_0}}\right); \quad \eta_a = \eta_{a0}\, e^{-\frac{c}{c_0}} + \eta_{a\infty}\left(1 - e^{-\frac{c}{c_0}}\right).$$

The quantum efficiencies of the donors and acceptors are η_{d0} and η_{a0} respectively when $c \to 0$ or when donors and acceptors are farther away from each other than R_0 (which has been shown to be realized with a probability of $e^{-\frac{c}{c_0}}$ for a Eu_2O_3 concentration of c). The quantum efficiencies are $\eta_{d\infty}$ and $\eta_{a\infty}$ for high concentrations, when both ion types certainly interact, or when they are within a distance smaller than R_0, (which has been shown to be realized with a probability of $1-e^{-\frac{c}{c_0}}$ for a Eu_2O_3 concentration of c). In our case, the energy transfer is only from $Eu^{3+}(C_{3i})$ to $Eu^{3+}(C_2)$. The quantum efficiency of the acceptors is therefore independent of concentration because this system can not lose excitation energy by transfer processes. Therefore we have for the acceptors $Eu^{3+}(C_2)$:

$$\eta_a=\eta_{a0} \quad \text{since} \quad \eta_{a\infty}=\eta_{a0}\,.$$

The quantum efficiency of the donors will decrease with increasing Eu_2O_3 concentration because this system will lose more and more excitation energy non-radiatively to the acceptors. Therefore we have for the donors $Eu^{3+}(C_{3i})$: $\eta_d=\eta_{d0}\, e^{-\frac{c}{c_0}}+\eta_{d\infty}(1-e^{-\frac{c}{c_0}})$.

In general $\eta_{d\infty} \ll \eta_{d0}$ will hold.

For the quantity f defined in (10) we get

$$f=\frac{\eta_d}{\eta_a}=\frac{\eta_d}{\eta_{a0}}=\frac{\eta_{d0}-\eta_{d\infty}}{\eta_{a0}}\, e^{-\frac{c}{c_0}}+\frac{\eta_{d\infty}}{\eta_{a0}}\,. \tag{12}$$

This expression has just the form introduced empirically in (11)

$$f=B\, e^{-\frac{c}{c_0}}+1-A \qquad \text{with } A=1-\frac{\eta_{d\infty}}{\eta_{a0}}\,. \tag{13}$$

If the energy transfer to the acceptors represents the only mechanism which decreases the quantum efficiency of the donors, then one can define the probability for energy transfer by

$$w_T=\frac{\eta_{d0}-\eta_d}{\eta_{d0}}=\left(1-\frac{\eta_{d\infty}}{\eta_{d0}}\right)(1-e^{-\frac{c}{c_0}})\,. \tag{14}$$

This is just the form of the expression (11), found empirically for w_T with a second value for $A=1-\frac{\eta_{d\infty}}{\eta_{d0}}$.

Both values for A are identical, if the difference between $\eta_{d\infty}/\eta_{a0}$ and $\eta_{d\infty}/\eta_{d0}$ can be neglected. It was not possible to differentiate between these two values by our experiments, since they have an error of $\pm 5\%$, and $\eta_{d\infty}$ is of the order 0.05 and η_{a0} and η_{d0} are both of the order of one. Indeed, one can take $\eta_{d0}=1$ as a good approximation if two conditions are fulfilled: first, the $^5D_1$ $Eu^{3+}(C_{3i})$ must decay solely by non radiative transitions to $^5D_0$ $Eu^{3+}(C_{3i})$, and, second, the $^5D_0$ $Eu^{3+}(C_{3i})$ must decay solely by radiative processes, i.e. must have a radiative efficiency of one.

Both can be assumed since no $^5D_1$ $Eu^{3+}(C_{3i})$ fluorescence could be found and the lifetime of 7.7 msec of $^5D_0$ $Eu^{3+}(C_{3i})$ agrees well with the calculated value for $M1$ transitions of 9.0 msec[9] indicating a radiative efficiency of nearly 100% for $^5D_0$ $Eu^{3+}(C_{3i})$. This is in contrast to $Eu^{3+}(C_2)$ where $^5D_1$ fluorescence can be observed clearly leading to $\eta_{a0}<1$. In this approximation one gets

$$w'_T=\frac{w_T}{\eta_{a0}}=\frac{1-\eta_{d\infty}}{\eta_{a0}}\left(1-e^{-\frac{c}{c_0}}\right),$$

$$f=\frac{1-\eta_{d\infty}}{\eta_{a0}}e^{-\frac{c}{c_0}}+\frac{\eta_{d\infty}}{\eta_{a0}}.$$

Extrapolating f for $c\to 0$ one gets the value η_{a0} needed for evaluating w_1 plotted in the figures from w'_T obtained by experiment (Eq. (6b)). The following relations hold between w'_T, w_T and f:

$$w'_T+f=\frac{1}{\eta_{a0}} \quad \text{or} \quad w_T+\eta_{a0}\cdot f=1.$$

These have been proved by the experiments to be valid at all three temperatures.

From the temperature independent parameter $c_0=(1.80\pm0.05)$ mol% Eu_2O_3 one gets the interaction range R_0

$$R_0=\sqrt[3]{\frac{1}{\pi c_0\cdot N_K}}=8.7\,\text{Å},$$

where $N_K=2.68\cdot10^{22}\,\text{cm}^{-3}$ is the density of Y^{3+} cation lattice sites. Within this sphere of radius R_0 there are 56 $Y^{3+}(C_2)$ lattice sites. The value of R_0 is comparable with the length of half the body diagonal of the unit cell (9.2 Å), and is more then twice as large as the shortest $Y^{3+}(C_{3i})-Y^{3+}(C_2)$ distance (3.52 Å).

The relatively small value of $R_0=8.7$ Å may be an indication that one is dealing with an exchange interaction, which must be phonon-assisted, since the interacting electronic levels are not in resonance. The latter is supported by the temperature dependence of the excitation spectrum of the $^5D_0$ $Eu^{3+}(C_{3i})$ fluorescence (Fig. 8). It shows the $Eu^{3+}(C_2)$ transitions more clearly at elevated temperatures indicating an increase of the reverse energy transfer from $Eu^{3+}(C_2)$ to $Eu^{3+}(C_{3i})$

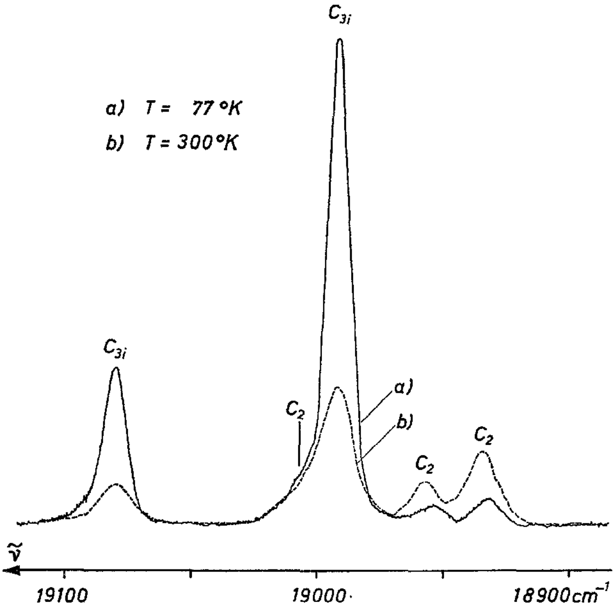

Fig. 8. Excitation spectra of the $^5D_0$ $Eu^{3+}(C_{3i})$ fluorescence line $\tilde{\nu}=17{,}170\,cm^{-1}$. a) $T=77$ °K; b) $T=300$ °K; $c=5.0$ mol% Eu_2O_3 in Y_2O_3

with increasing temperature which can take place only by phonon absorption.

In order to clarify the quantum mechanical process governing the energy transfer and deciding whether the transfer is between the $^5D_0$ or $^5D_1$ states of both ions, further experiments are needed, especially time resolved measurements of the fluorescence decay, the results of which will be published soon.

The work was carried out under the "Sonderforschungsbereich Festkörperspektroskopie Darmstadt-Frankfurt".

J. Heber
K. H. Hellwege
U. Köbler
H. Murmann
Institut für Technische Physik
der T.H. Darmstadt
D-6100 Darmstadt, Hochschulstraße